

Article

# A Biologically-Inspired Power Control Algorithm for Energy-Efficient Cellular Networks

Hyun-Ho Choi <sup>1</sup> and Jung-Ryun Lee <sup>2,\*</sup>

<sup>1</sup> Department of Electrical, Electronic and Control Engineering,  
Institute for Information Technology Convergence, Hankyong National University,  
327 Chungang-ro, Anseong 17579, Korea; hhchoi@hknu.ac.kr

<sup>2</sup> School of the Electrical Engineering, Chung-Ang University, 84 Heukseok-ro, Dongjak-gu,  
Seoul 06974, Korea

\* Correspondence: jrlee@cau.ac.kr; Tel.: +82-2-820-5820; Fax: +82-2-824-2371

Academic Editor: Luca Chiaraviglio

Received: 9 December 2015; Accepted: 26 February 2016; Published: 4 March 2016

**Abstract:** Most of the energy used to operate a cellular network is consumed by a base station (BS), and reducing the transmission power of a BS can therefore afford a substantial reduction in the amount of energy used in a network. In this paper, we propose a distributed transmit power control (TPC) algorithm inspired by bird flocking behavior as a means of improving the energy efficiency of a cellular network. Just as each bird in a flock attempts to match its velocity with the average velocity of adjacent birds, in the proposed algorithm, each mobile station (MS) in a cell matches its rate with the average rate of the co-channel MSs in adjacent cells by controlling the transmit power of its serving BS. We verify that this bio-inspired TPC algorithm using a local rate-average process achieves an exponential convergence and maximizes the minimum rate of the MSs concerned. Simulation results show that the proposed TPC algorithm follows the same convergence properties as the flocking algorithm and also effectively reduces the power consumption at the BSs while maintaining a low outage probability as the inter-cell interference increases; in so doing, it significantly improves the energy efficiency of a cellular network.

**Keywords:** power control algorithm; energy efficiency; green base station; bio-inspired algorithm; flocking model; energy-efficient cellular network

---

## 1. Introduction

The worldwide reduction of energy consumption, and therefore of greenhouse gas emissions, is now one of the most urgent challenges of our age. At the same time, the rapid growth in wireless communication networks requires huge amounts of energy to provide wide bandwidths for numerous mobile devices. With the rapid growth of the mobile market, service providers have increased the number of base stations (BSs) in an attempt to attract more subscribers. However, most of the energy used to operate a cellular network is consumed by BSs, and service providers therefore require energy-efficient BSs in order to reduce their operational expenditure. BSs consume energy in three operational functions: in radio transmission, in baseband processing and in the feeder. Among these, the radio part consumes more than 80% of the energy of a BS to amplify the transmitting signal [1–3]. Therefore, reducing the transmission power of the BS could yield a substantial energy savings in the cellular network.

It has been recognized that a tradeoff exists between the energy consumed at a transmitter and the signal quality at a receiver (e.g., data rate or outage probability) according to the allocated transmission power [4–8]. Considering this tradeoff, many authors have tried to minimize energy consumption while satisfying the required signal quality by controlling the transmission power. Long-term transmit

power control (TPC) algorithms, known as a “cell-breathing” or a “cell-zooming” technique, have been proposed to minimize the energy consumption of a BS according to variations in the traffic load with a certain cell throughput constraint [9–11]. In these schemes, a cell experiencing a heavy load or interference reduces its size by decreasing the transmission power of the BS, while neighboring cells cover those users who cannot be served by the overloaded cell, by increasing the transmission power of the BS. Furthermore, signal-to-interference plus noise ratio (SINR)-based TPC algorithms use the minimum transmit power level necessary to guarantee the required SINR at the receiving node, in an attempt to achieve not only interference mitigation, but also power savings [12–14]. Similarly, the transmit power is minimized based on channel state information (CSI) while maintaining a constant outage probability or bit error rate (BER) at the receiver under fading environments [15–19]. Moreover, an optimized transmit power is derived at each BS to maximize the overall network capacity under a quality of service (QoS) constraint, such that energy efficiency is improved [20–23]. Furthermore, recently, the joint power control and resource allocation problems in heterogeneous cellular networks have been investigated, and the practical distributed subchannel and power allocation algorithms have been developed in order to improve the network capacity and the user fairness [24–26].

As reviewed above, a common strategy used by most TPC algorithms is to minimize the transmit power consumption while ensuring the required QoS (*i.e.*, SINR, rate or BER) of each mobile station (MS) [12–19]. This strategy provides satisfactory operation in low interference environments. However, if the interference level increases, the transmission power must increase, eventually reaching a maximum value. In this case, an outage (*i.e.*, where the required QoS is violated) may occur even though a high transmission power is used. Therefore, the power minimization approach that is subject to a constant SINR requirement is somewhat constrained in such an interference-limited environment. Moreover, in this power minimization method, the target SINR is a key parameter that closely affects both QoS performance and energy efficiency. However, it is difficult to determine an appropriate target SINR according to the interference level, because this requires a complex calculation and a significant overhead for sharing channel information between all MSs and all BSs [12–14]. In addition, the conventional TPC algorithms in cellular networks mostly require a centralized controller that gathers the necessary channel information from other nodes, calculates the appropriate power level or the target SINR value and informs each node of the determined parameters [15–23]. This induces a large overhead for exchanging control information among network entities and requires a high complexity to calculate the operational parameters.

To solve this TPC problem, in this paper, we refer to the biological phenomenon known as *flocking behavior*, which is exhibited when a group (or flock) of birds are in flight together [27]. Flocks behave with very simple rules, even in complex and dynamically-changing environments, showing emergent behavior to achieve a common goal, maximizing the minimum velocity of birds in a group in a robust and efficient manner. With the understanding of the similarities between flocking behavior and TPC in a cellular network, we make use of the underlying principles of flocking behavior in our TPC algorithm. Specifically, the proposed TPC algorithm adopts a local rate-averaging algorithm inspired by the flocking behavior in order to control the transmission power of BSs. Just as the flocking algorithm operates in a simple and distributed manner and shows convergent phenomena, our proposed bio-inspired TPC algorithm operates with a low level of complexity without a centralized controller and shows that the transmit powers of the BSs uniformly converge and that the rates of the MSs converge to the same value that maximizes the minimum rate. This eventually leads to a decrease in the energy consumption of the BS while lowering the outage probability of the MS in the wireless cellular network with a dynamically-changing interference level.

The remainder of this paper is organized as follows. In Section 2, we present the system model for the considered problem. In Section 3, we introduce the flocking model and discuss its properties as they are currently understood. In Section 4, we explain the details of the proposed TPC algorithm, and in Section 5, we analyze the proposed TPC algorithm in mathematical terms. In Section 6, we discuss the simulation results, and finally, we offer some conclusions in Section 7.

## 2. System Model

We consider a cellular system with a finite number of channels (a frequency or a time slot), and the channels are fully reused in every cell. We denote the number of BSs by  $N$ . Then, the number of MSs using the same channel (*i.e.*, co-channel MSs) becomes  $N$  assuming that each channel is allocated to a certain MS in each cell by an arbitrary channel assignment scheme (for example, the random channel assignment can be used [28]; the resource allocation scheme is beyond the scope of this paper). In general terms, MS  $i$  is served by the BS  $i$  that is closest to it for communication.  $P_i$  denotes the transmit power of BS  $i$ , and  $n_i$  denotes the noise power at MS  $i$ .  $G_{ij}$  denotes the channel gain of the communication link from BS  $j$  to MS  $i$ . This is illustrated in Figure 1. Then, the SINR of MS  $i$  is expressed as:

$$\gamma_i = \frac{G_{ii}P_i}{\sum_{j=1, j \neq i}^N G_{ij}P_j + n_i}, \quad 1 \leq i \leq N \quad (1)$$

From Shannon's theorem, the bit rate of MS  $i$  per unit bandwidth (or spectral efficiency) in bits/second/Hz is given by:

$$R_i = \log_2(1 + \gamma_i) \text{ b/s/Hz} \quad (2)$$

In addition, we define the outage probability of MS  $i$  to be the probability that the received SINR  $\gamma_i$  falls below the required SINR,  $\gamma_{req}$ , as follows:

$$\mathcal{P}_i^{out} := Pr\{\gamma_i < \gamma_{req}\} \quad (3)$$

Finally, we define the energy efficiency of MS  $i$  as the number of information bits transmitted without error per unit bandwidth and per unit energy in units of bits/Hz/Joule. Because the occurrence of outage induces bit error, the energy efficiency is defined as [11]:

$$E_i := \frac{(1 - \mathcal{P}_i^{out})R_i}{P_i} \text{ [b/Hz/J]} \quad (4)$$

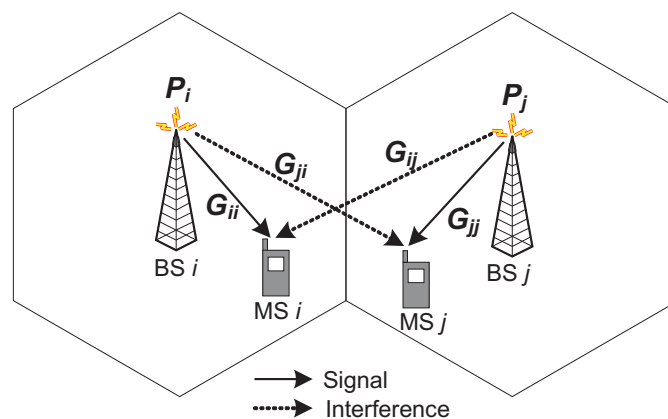


Figure 1. Channel gain of the communication link in the two-cell case.

## 3. Flocking Behavior

Flocking represents the phenomenon in which self-propelled individuals organize themselves into an ordered motion using only limited environmental information and a simple set of rules. For example, a flock of birds whose members are moving in  $\mathbb{R}^3$  shows that the state of the flock converges to one in which all birds fly with the same velocity. The simple rule governing this flocking behavior is known, that each bird autonomously adjusts its velocity according to the velocities of its

neighbors. The representative Cucker–Smale flocking model explains this flocking behavior; in other words at time  $t$  and for bird  $i$ , each bird adjusts its velocity  $v_i$  as follows [27]:

$$v_i(t+1) - v_i(t) = \frac{\lambda}{N} \sum_{j=1}^N \psi(|x_j - x_i|)(v_j(t) - v_i(t)) \quad (5)$$

where  $N$  is the number of birds,  $\lambda \leq 1$  is a coupling strength used as a learning parameter and  $x_i$  is the position of bird  $i$  in  $\mathbb{R}^3$ .  $\psi$  denotes a communication range function depending on the distance between two birds. For example, it is defined as  $\psi(|x_j - x_i|) = 1$  only if  $|x_j - x_i| \leq r$  in which  $r$  is the visible range of a bird. In this case, the flocking model can be interpreted as a local-averaging algorithm for bird velocity. Furthermore, Cucker and Smale have proven that an interacting  $N$ -particle system  $\{(x_i(t), v_i(t))\}_{i=1}^N$  under the control of Equation (5) has time-asymptotic convergence properties if  $\psi$  is a non-negative and non-increasing function, as follows [27]:

(1) Velocity alignment:

$$\lim_{t \rightarrow \infty} |v_i(t) - v_j(t)| = 0, \text{ for } \forall i \neq j \quad (6)$$

(2) Formation of a group:

$$\sup_{0 \leq t < \infty} |x_i(t) - x_j(t)| < \infty, \text{ for } \forall i \neq j \quad (7)$$

On the other hand, one reason why birds form into flocks is that there is an aerodynamic advantage to flying behind other birds in a coordinated flight [29]. As the front bird moves its wings up and down, a strong current of air is created, which flows backwards relative to this bird. This moving wave of air lifts the bird behind it. In other words, each flying bird creates a wave of air pressure that helps the bird flying behind it. This cooperation reduces the energy consumption of the birds and, thus, allows them to arrive at their destination more quickly [30]. Because of these aerodynamic interactions among the birds, the best way for a bird group to arrive at its destination as quickly as possible without stragglers (*i.e.*, to maximize the speed of the slowest bird) is for them to cooperate in such a way that the speedier birds fly in front of the slower birds. This cooperation causes all birds to fly at the same velocity, which eventually maximizes the minimum speed of the flock and reduces its energy consumption.

#### 4. Proposed Bio-Inspired Transmit Power Control Algorithm

Both the considered TPC algorithm and the flocking behavior described above allow the pursuit of the same objective of the *max-min* type in an interactive environment. Just as a flock of birds aims to maximize the minimum bird speed in an aerodynamic interactive environment, our proposed TPC algorithm is designed to maximize the minimum rate of the MSs in an inter-cell interference environment. Therefore, the proposed TPC algorithm controls the transmit power of each BS in such a way as to equalize the rates of all of the MSs (*i.e.*,  $R_i = R_j, \forall i, j$ ). Because the rate of MS  $i$  ( $R_i$ ) is related to the transmit powers of all of the other BSs ( $P_j, \forall j \neq i$ ), as well as to the transmit power of its serving BS  $i$  ( $P_i$ ), controlling the transmit power of one BS influences the rates of all of the other MSs; an iteration is therefore required to obtain the final equal rate value just as in the flocking algorithm. At each step, each MS recognizes the rate information of the other MSs from its neighboring BSs and sets its next target rate to the average of the the recognized rate values, just as each bird in a flock adjusts its velocity to the average velocity of its neighbors. Following the feedback of this target rate from the MS to its serving BS, the BS determines its transmit power to achieve the target rate individually. This distributed local rate-average operation is repeated until the target rate does not change any more (*i.e.*, until all of the MS rates converge to the same value).

Figure 2 shows the flow chart of the proposed TPC algorithm. Its operational procedure follows these steps:

1. The serving BS  $i$  sets the transmit power to the maximum value  $P_{max}$  at the initial time.
2. BS  $i$  sends the data packet to its MS  $i$  using the transmit power  $P_i(t)$  determined for time  $t$ .
3. On receiving the packet, MS  $i$  measures its SINR  $\gamma_i$ .
4. MS  $i$  calculates its current rate as  $R_i(t) = \log_2(1 + \gamma_i(t))$ .
5. MS  $i$  overhears the rate information  $R_j(t)$  of the adjacent MS  $j$  from its neighboring BSs  $j \neq i$  (generally, in cellular systems, the rate value is mapped to one of the modulation and coding sets (MCS), and the MCS value corresponding to the data channel is broadcast through a common control channel [31]; because this broadcast common control channel is modulated by the most robust MCS level, the MS can overhear it after just synchronization to the adjacent cell and then discover the rate information of the corresponding data channel [32]; moreover, it is worth noting that the direct wired communication among BSs is also possible for sharing the rate information, instead of the overhearing technique).
6. The MS  $i$  calculates the next target rate  $R_i(t + 1)$  as:

$$R_i(t + 1) - R_i(t) = \frac{\lambda}{N} \sum_{j=1}^N \psi(|x_j - x_i|) (R_j(t) - R_i(t)) \quad (8)$$

which follows the same form as Equation (5) (note that Equations (5) and (8) have a similar form to one of the consensus protocols, so they can also be interpreted as the decentralized consensus protocol [33]). The only difference is that the velocity of bird  $v$  is replaced by the rate of MS  $R$ . Similarly,  $\psi(|x_j - x_i|)$  is the communication range function where  $x_j$  and  $x_i$  are the positions of BS  $j$  and MS  $i$ , respectively. Here, we assume that  $\psi(|x_j - x_i|) = 1$  if the physical distance between two stations is less than the overhearing range  $r$ , i.e.,  $|x_j - x_i| \leq r$ . Otherwise,  $\psi(|x_k - x_i|) = 0$ . If we choose  $\lambda = 1$ , then Equation (8) is re-expressed as:

$$R_i(t + 1) = \frac{1}{|N_i|} \sum_{j \in N_i} R_j(t) \quad (9)$$

where  $N_i$  is the set of neighboring BSs overheard by MS  $i$  and  $|\cdot|$  is the cardinality of a set. Clearly, this is a distributed local averaging algorithm for the rates of the MSs.

7. If there is little difference between the next target rate  $R_i(t + 1)$  and the current rate  $R_i(t)$  (i.e.,  $R_i(t + 1) - R_i(t) < \epsilon$  where  $\epsilon > 0$  is sufficiently small), MS  $i$  sends no feedback. Otherwise, it feeds back the received SINR  $\gamma_i(t)$  and the next target rate  $R_i(t + 1)$  to its serving BS  $i$ .
8. If BS  $i$  receives feedback from MS  $i$ , it calculates its next transmit power  $P_i(t + 1)$  to achieve the next target rate  $R_i(t + 1)$  using the following relationship:

$$\begin{aligned} R_i(t + 1) &= \log_2(1 + \tilde{\gamma}_i(t + 1)) \\ &= \log_2 \left( 1 + \frac{G_{ii}P_i(t + 1)}{\sum_{j=1, j \neq i}^N G_{ij}P_j(t) + n_i} \right) \\ &= \log_2 \left( 1 + \frac{\gamma_i(t)}{P_i(t)} \cdot P_i(t + 1) \right) \end{aligned} \quad (10)$$

where  $\tilde{\gamma}_i(t + 1)$  is the estimated SINR of MS  $i$  to be used at time  $t + 1$ . From Equation (10), we can determine the next transmit power of BS  $i$  at time  $t + 1$ , as follows.

$$P_i(t + 1) = \min \left[ P_{max}, \left( 2^{R_i(t+1)} - 1 \right) \frac{P_i(t)}{\gamma_i(t)} \right] \quad (11)$$

If the BS  $i$  does not receive the feedback, it preserves its previous transmit power.

**Remark 1.** As seen in (11), the BS needs only  $R_i(t + 1)$  and  $\gamma_i(t)$  information to determine its next transmit power. This significantly reduces the feedback overhead compared to the conventional centralized power control schemes [34].

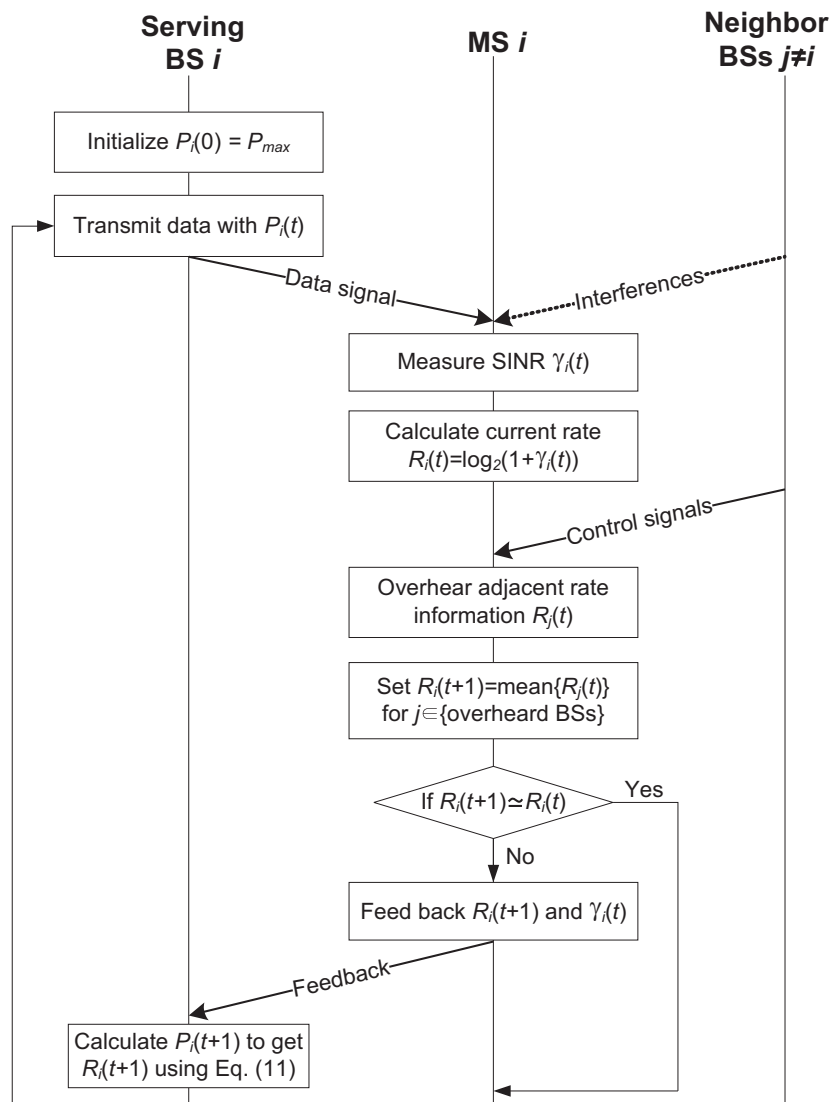


Figure 2. Flow chart of the proposed transmit power control (TPC) algorithm.

### 5. Analysis of the Proposed TPC Algorithm

In this section, we analyze the proposed bio-inspired TPC algorithm with respect to its convergence and its achievability to maximize the minimum rate of MSs.

#### 5.1. Convergence

To analyze the convergence performance of the proposed TPC algorithm, we consider the continuous time version of Equation (8) as:

$$\frac{dR_i(t)}{dt} = \frac{\lambda}{N} \sum_{j=1}^N \psi(|x_j - x_i|) (R_j(t) - R_i(t)) \tag{12}$$

We denote the center of  $R_i(t)$  as  $R_c(t)$ , which is given by:

$$R_c(t) = \frac{1}{N} \sum_{i=1}^N R_i(t) \tag{13}$$

By differentiating Equation (13), we obtain:

$$\begin{aligned} \frac{dR_c(t)}{dt} &= \frac{1}{N} \sum_{i=1}^N \frac{dR_i(t)}{dt} \\ &= \frac{\lambda}{N^2} \sum_{i=1}^N \sum_{j=1}^N \psi(|x_j - x_i|) (R_j(t) - R_i(t)) \\ &= \frac{\lambda}{2N^2} \left\{ \sum_{i=1}^N \sum_{j=1}^N \psi(|x_j - x_i|) (R_j(t) - R_i(t)) + \sum_{j=1}^N \sum_{i=1}^N \psi(|x_i - x_j|) (R_i(t) - R_j(t)) \right\} \\ &= \frac{\lambda}{2N^2} \sum_{i=1}^N \sum_{j=1}^N \psi(|x_j - x_i|) (R_j(t) - R_j(t) + R_i(t) - R_i(t)) \\ &= 0 \end{aligned} \tag{14}$$

From Equation (14), we obtain the explicit solution  $R_c(t) = R_c(0)$ .

We now define a new variable  $\hat{R}_i(t)$  by shifting  $R_i(t)$  by  $R_c(0)$  to see the fluctuation of  $R_i(t)$  around the center  $R_c(0)$ , which is given by:

$$\hat{R}_i(t) := R_i(t) - R_c(0) \tag{15}$$

From Equations (13) and (15), we have:

$$\sum_{i=1}^N \hat{R}_i(t) = 0 \tag{16}$$

Thereafter, we define a set  $\mathbf{R}(t) := \{\hat{R}_1(t), \hat{R}_2(t), \dots, \hat{R}_N(t)\} \in \mathbb{R}^N$ . As a quantity proportional to the standard deviation of  $\mathbf{R}(t)$ , we consider its  $L^2$  norm given by  $\|\mathbf{R}\| = \sqrt{\sum_{i=1}^N |\hat{R}_i|^2}$ .

Applying Equations (15) to (12), we first obtain:

$$\begin{aligned} \frac{d|\hat{R}_i(t)|^2}{dt} &= 2\hat{R}_i(t) \cdot \frac{d|\hat{R}_i(t)|}{dt} \\ &= 2\hat{R}_i(t) \cdot \frac{\lambda}{N} \sum_{j=1}^N \psi(|x_j - x_i|) (\hat{R}_j(t) - \hat{R}_i(t)) \end{aligned} \tag{17}$$

Then, we calculate the derivative of  $\|\mathbf{R}\|^2$  as:

$$\begin{aligned} \frac{d\|\mathbf{R}\|^2}{dt} &= \frac{d}{dt} \sum_{i=1}^N |\hat{R}_i|^2 = \sum_{i=1}^N \frac{d|\hat{R}_i|^2}{dt} \\ &= \frac{\lambda}{N} \sum_{i=1}^N 2\hat{R}_i \sum_{j=1}^N \psi(|x_j - x_i|) (\hat{R}_j - \hat{R}_i) \\ &= -\frac{\lambda}{N} \sum_{i=1}^N \sum_{j=1}^N \psi(|x_j - x_i|) (2\hat{R}_i^2 - 2\hat{R}_i\hat{R}_j) \\ &= -\frac{\lambda}{N} \sum_{i=1}^N \sum_{j=1}^N \psi(|x_j - x_i|) |\hat{R}_j - \hat{R}_i|^2 \end{aligned} \tag{18}$$



Let  $x_{max} = \max_{i,j} |x_j - x_i|$ . Because  $\psi$  is a non-negative and non-increasing function, we further develop Equation (18) as:

$$\begin{aligned}
 \frac{d\|\mathbf{R}\|^2}{dt} &\leq -\frac{\lambda}{N} \sum_{i=1}^N \sum_{j=1}^N \psi(x_{max}) |\hat{R}_j - \hat{R}_i|^2 \\
 &= -\frac{\lambda}{N} \psi(x_{max}) \sum_{i=1}^N \sum_{j=1}^N (\hat{R}_j^2 + \hat{R}_i^2 - 2\hat{R}_j\hat{R}_i) \\
 &= -\frac{\lambda}{N} \psi(x_{max}) \left( \sum_{i=1}^N \sum_{j=1}^N 2\hat{R}_i^2 - 2 \sum_{i=1}^N \hat{R}_i \sum_{j=1}^N \hat{R}_j \right) \\
 &= -\frac{\lambda}{N} \psi(x_{max}) (2N\|\mathbf{R}\|^2 - 0) \\
 &= -2\lambda\psi(x_{max})\|\mathbf{R}\|^2
 \end{aligned} \tag{19}$$

By solving this differential equation, we obtain:

$$\|\mathbf{R}(t)\|^2 \leq \|\mathbf{R}(0)\|^2 e^{-2\lambda\psi(x_{max})t} \tag{20}$$

$$\therefore \|\mathbf{R}(t)\| \leq \|\mathbf{R}(0)\| e^{-\lambda\psi(x_{max})t} \tag{21}$$

which proves that the proposed TPC algorithm achieves exponential convergence.

## 5.2. Achievability of the Max-Min Rate

In the cellular network, the rate set of wireless links that use the same channel at the same time affect each other owing to their inter-cell interferences [35]. It is therefore always possible to increase the rate of one link at the expense of another. Here, we term this property *solidarity* and define it as follows.

**Definition 1** (Solidarity Property). *A subset  $\mathcal{X}$  of  $\mathbb{R}^n$  has solidarity if and only if for all  $i \in \{1, 2, \dots, n\}$ , for all  $\mathbf{x} \in \mathcal{X}$ , where the  $i$ -th element  $x_i > 0$ , and for all  $0 < \alpha_i < \epsilon$ , where  $\epsilon > 0$  is small enough, the variation in  $x_i$ ,  $x_i \pm \alpha_i$ , induces variations in the other elements,  $x_j \mp \alpha_j$  for  $\forall j \neq i$  and  $0 < \alpha_j < \epsilon$ , and the changed vector  $\mathbf{y} = \mathbf{x} \pm \alpha_i \mathbf{e}_i \mp \sum_{j \neq i} \alpha_j \mathbf{e}_j$ , where  $\mathbf{e}_i$  is a unit vector, still belongs to  $\mathcal{X}$ .*

In other words, the solidarity property exists if a small increase and decrease in one element causes a small decrease and increase in all of the other elements. According to the definition of solidarity, we make the following proposition and prove it in order to verify that the proposed TPC algorithm maximizes the minimum rate of the co-channel MSs.

**Proposition 1.** *If a set  $\mathcal{X}$  has the solidarity property, then all of the components of the max-min fair vector  $\mathbf{x} \in \mathcal{X}$  are equal, i.e.,  $x_i = x_j$  for  $\forall i, j$  when the minimum value of  $\mathbf{x}$  is maximized.*

**Proof.** Suppose on the contrary that there exists a max-min fair vector  $\mathbf{x}$ , such that  $x_i \neq x_j$  for some  $i \neq j$  on  $\mathcal{X}$  with the solidarity property. Let  $x_i$  be the largest component of  $\mathbf{x}$ . Then, for sufficiently small  $\epsilon$ , such that  $0 < \epsilon < \min_j \{x_i - x_j\}$ , we have:

$$x_i > x_j + \epsilon \text{ for } \forall j \neq i \tag{22}$$

According to the definition of the solidarity property, for  $0 < \alpha_i, \alpha_j < \epsilon$ , we can find another vector  $\mathbf{y} \in \mathcal{X}$ , such that:

$$\mathbf{y} = \mathbf{x} - \alpha_i \mathbf{e}_i + \sum_{j \neq i} \alpha_j \mathbf{e}_j \tag{23}$$



That is,  $y_i = x_i - \alpha_i$  and  $y_j = x_j + \alpha_j$  for  $\forall j \neq i$ . This satisfies  $y_i > x_i - \epsilon > x_j$  and  $y_j > x_j$  for  $\forall j \neq i$ . Therefore, all elements of  $\mathbf{y}$  are greater than  $x_j$ , *i.e.*,

$$\max\{\min(\mathbf{y})\} > \max\{\min(\mathbf{x})\} = x_j \quad (24)$$

which contradicts the supposition that  $\mathbf{x}$  is the max-min fair vector.  $\square$

Due to inter-cell interference, the rate set of co-channel MSs in the cellular network has the solidarity property. As a consequence, from Proposition 1, the minimum rate of co-channel MSs is maximized when the rates of all of these MSs are equal. Therefore, the proposed TPC algorithm, which controls the transmit power of each BS in such a way as to equalize the rates of all of the MSs, maximizes the minimum rate of the MSs.

## 6. Results and Discussion

Table 1 summarizes the simulation parameters used in our study. We consider a hexagonal multi-cell layout where the distance between adjacent BSs is 500 m and an MS is positioned randomly in each cell. Considering a multi-tier cell structure, the number of BSs varies up to 20. The maximum transmit power, the path loss and fading models and the noise figure are all based on the 3GPP evaluation methodology [36]. We also set the required SINR to 0 dB, which is generally used as the threshold to decode the received signal in cellular networks. We assume that there is no error or delay in overhearing the rate information from the neighbor BSs. We perform a Monte Carlo simulation 10,000 times using MATLAB. For comparison, we also consider a scheme using maximum equal power without TPC and the SINR-based TPC algorithm with several target SINR values, in which each BS controls its transmission power in order that the received SINR satisfies a given target SINR [12–14].

**Table 1.** Parameter setup. MS, mobile station.

Parameter	Value
Cell layout	Hexagonal, one sector per cell
Number of BSs	3~20
Inter-BS distance	500 m
MS layout	Uniform in hexagonal cell
Maximum BS transmit power	46 dBm
Distance-dependent path loss	$128.1 + 37.6 \log_{10} R$ (dB), $R$ in km
Shadowing model	Log-normal with standard deviation of 8 dB
Fast fading model	Rayleigh
Noise figure	9 dB
Channel bandwidth allocated to an MS	100 kHz
Required SINR ( $\gamma_{req}$ )	0 dB
Coupling strength ( $\lambda$ )	1
Overhearing range ( $r$ )	500~900 m
Threshold for convergence check ( $\epsilon$ )	$10^{-4}$
Simulation trials	10,000

Figure 3 shows the received signal strength (RSS) in a two-dimensional plane when the maximum equal power allocation and the proposed TPC algorithm are used in a seven-cell topology. Here, the black points in cells indicate the position of the MSs using the same channel. The transmit power of each BS and the rate of each MS are displayed in each cell. The maximum equal power allocation scheme shows a uniform RSS distribution and a variety of different rates, but the proposed TPC algorithm shows a dynamic RSS distribution (*i.e.*, different transmit powers) and the same rate across all of the cells. It is notable that in this example, the proposed TPC algorithm increases the minimum

MS rate from 1.58 to 3.47 b/s/Hz, while using 5.29 dB less transmit power compared to the maximum equal power allocation.

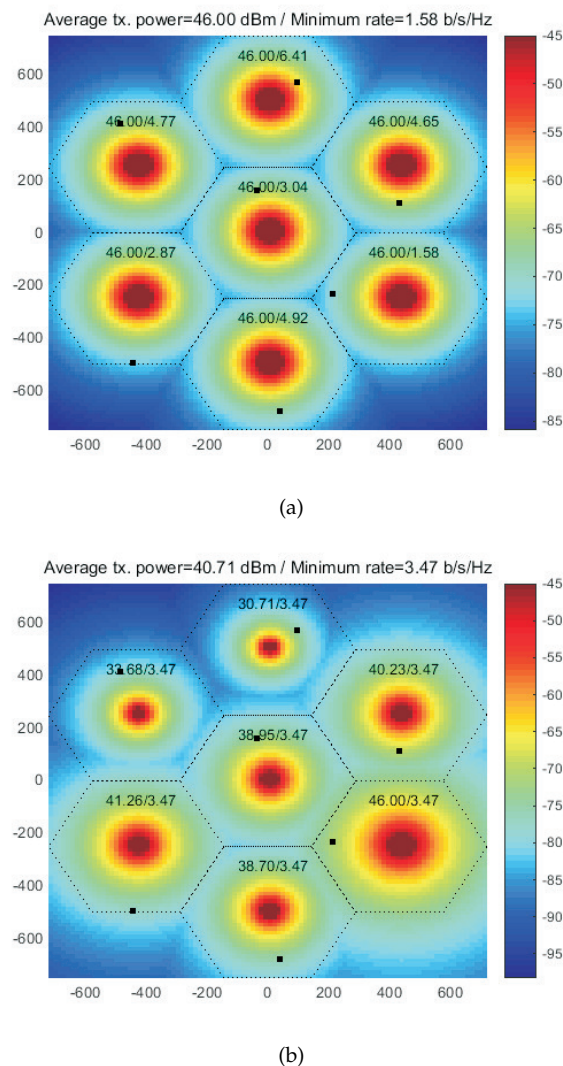
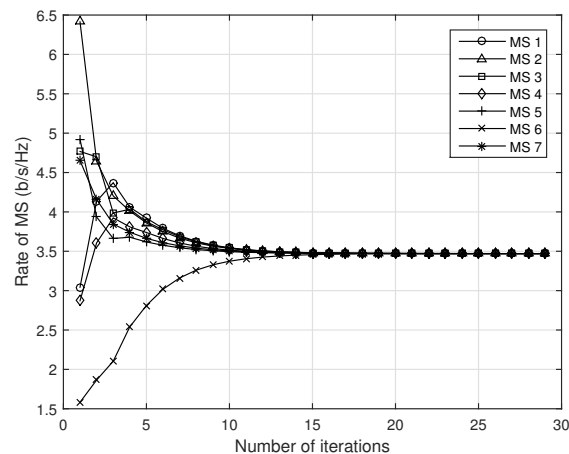
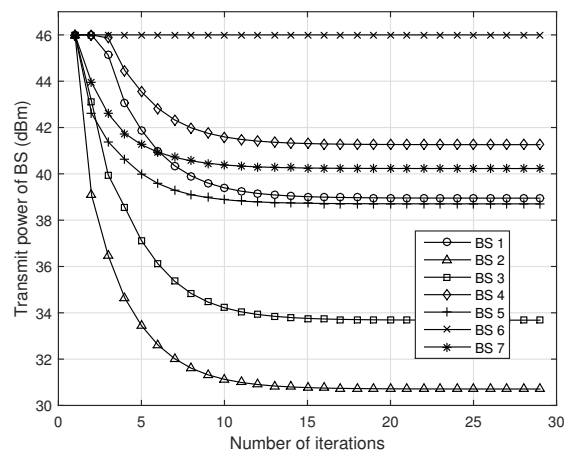


**Figure 3.** Distribution of received signal strength in two dimensions: (a) maximum equal power allocation; and (b) proposed TPC algorithm.

Figure 4 shows the rate of each MS and the transmit power of each BS according to the iteration of the proposed algorithm in the same seven-cell topology as in Figure 3. As the iteration proceeds, all of the MS rates converge to the same value, and the maximum difference of transmit powers of the BSs is uniformly bounded. These results can be expressed as  $\lim_{t \rightarrow \infty} |R_i(t) - R_j(t)| = 0$  for  $\forall i \neq j$  and  $\sup_{0 \leq t < \infty} |P_i(t) - P_j(t)| < P_{max}$  for  $\forall i \neq j$ , which correspond to the convergence properties of the flocking algorithm shown in Equations (6) and (7), respectively. Upon convergence, the MS that had the best rate initially (*i.e.*, MS 2) makes its serving BS 2 use the lowest transmit power, but the MS that had the worst rate initially (*i.e.*, MS 6) lets its serving BS 6 maintain the maximum transmit power. In other words, MSs with a good link quality reduce the transmit power of their serving BSs, while MSs with a poor link quality maintain or slightly reduce the transmit power of their serving BSs in order to equalize the rates of all of the MSs. Thanks to the altruistic nature of this arrangement, the final transmit power is inversely proportional to the initial rate of the MS.



(a)



(b)

**Figure 4.** (a) Rate of MS; and (b) transmit power of BS *vs.* number of iterations.

Figure 5 shows the number of iterations needed for convergence as functions of the number of BSs and the overhearing range ( $r$ ). As the number of BSs increases, the number of iterations increases, because the amount of rate information to be considered in the algorithm increases. The MS can overhear the rate information only from those BSs located within the overhearing range. Therefore, the number of iterations increases as the overhearing range decreases, because less rate information is offered to the algorithm for averaging. Here, we assume that the algorithm has converged if the rate differences in time  $|R_i(t+1) - R_i(t)|$  are less than  $10^{-4}$  for  $\forall i$ . However, this convergence condition is a tight one because in practical systems, the rate does not have a real value, but a discrete one, as one of the predetermined MCS levels. Thus, this convergence time can be decreased according to the granularity of the rate information.

Figure 6 shows the performance of the minimum rate of the MSs *versus* the number of BSs. As the number of BSs increases, the minimum rate in all of the schemes decreases exponentially because the increased number of BSs causes more inter-cell interferences. The proposed TPC algorithm outperforms the scheme using the maximum equal power without TPC and an SINR-based TPC algorithm with a target SINR ( $\theta$ ) of 0, 3 or 10 dB. This is because the proposed TPC algorithm dynamically achieves an SINR value that maximizes the minimum rate regardless of the interference level, while the SINR-based TPC algorithm always tries to achieve a static target SINR. The SINR-based TPC algorithm shows that there exists a suitable target SINR according to the number of BSs (*i.e.*, interference level).

The maximum equal power scheme has the lowest minimum rate, because it does not adjust the transmit power in consideration of the inter-cell interference situation.

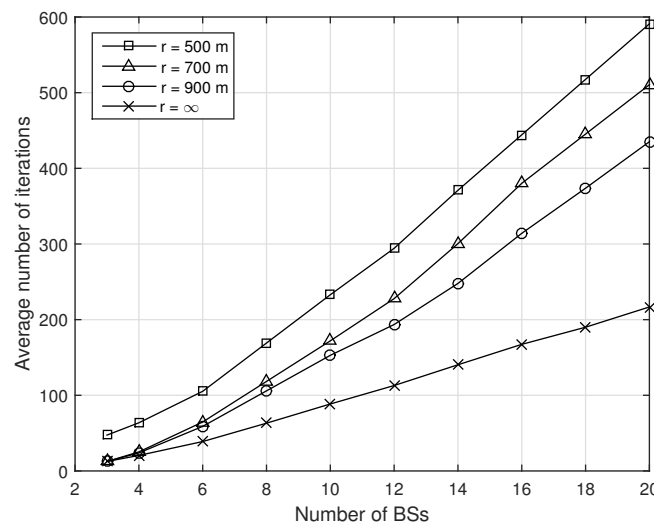


Figure 5. Number of iterations *vs.* number of BSs and overhearing range ( $r$ ).

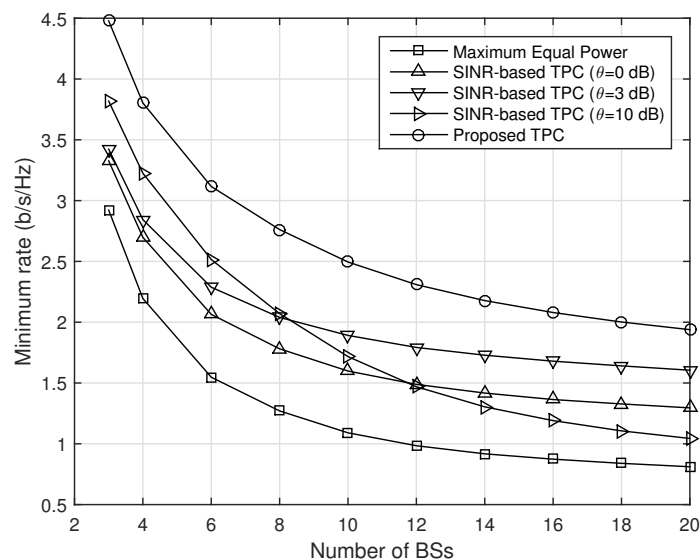


Figure 6. Minimum rate *vs.* number of BSs.

Figure 7 shows the average transmission power at the BSs *versus* the number of BSs. As the number of BSs increases, the inter-cell interference increases, and so, the proposed TPC algorithm reduces the transmission power more in order to reduce the interference to the MSs that receive the strong interference. In particular, the proposed TPC reduces the transmit power adaptively depending on the interference level; therefore, it exhibits a lower power consumption than the other schemes as the interference level increases. On the other hand, the SINR-based TPC algorithm consumes a higher transmission power at a high interference level and also shows that an appropriate target SINR value varies with the interference level.

Figure 8 shows the outage probability *versus* the number of BSs when the required SINR threshold  $\gamma_{req}$  is 0 dB. The SINR-based TPC with  $\theta = 0$  dB has the lowest outage probability, because its target SINR is set equal to the required SINR threshold. Apart from this, the proposed TPC shows the lowest outage probability. This implies that the proposed TPC algorithm almost satisfies the target SINR in a

way adaptive to the change in interference level, even though it uses significantly lower transmission power than the other schemes. On the other hand, the SINR-based TPC with a high target SINR and the maximum equal power scheme show a much higher outage probability, because they cause more severe interferences to MSs with low SINR.

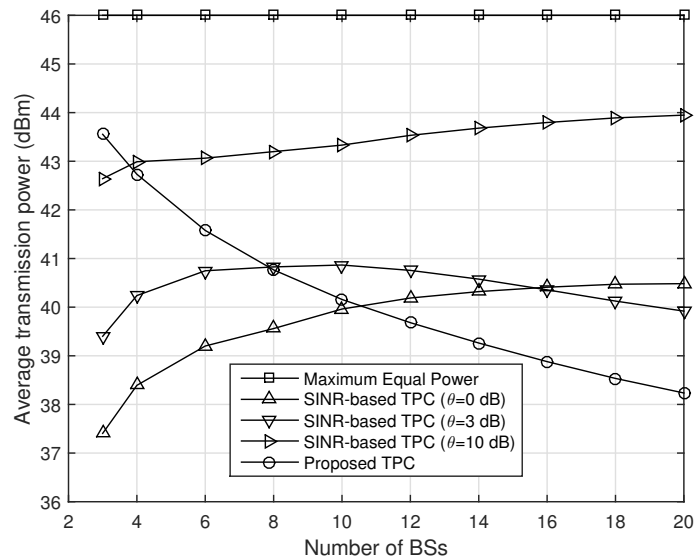


Figure 7. Average transmission power vs. number of BSs.

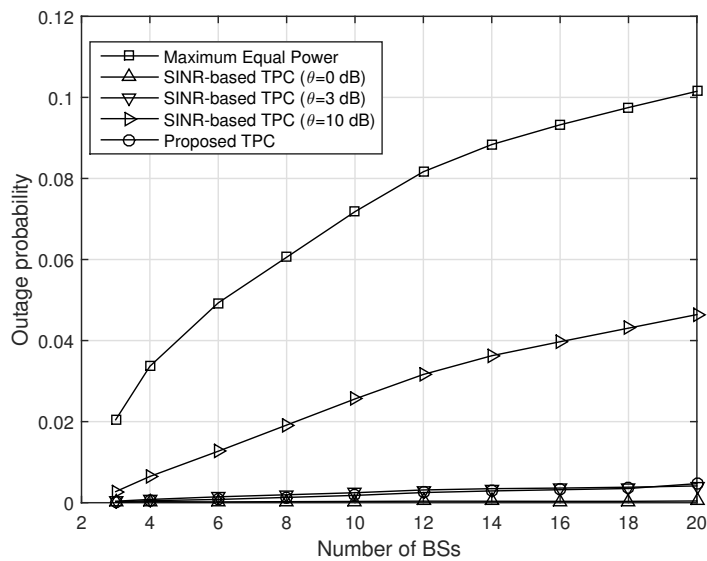


Figure 8. Outage probability power vs. number of BSs when  $\gamma_{req} = 0$  dB.

Figure 9 shows the energy efficiency versus the number of BSs. The energy efficiency indicates the number of data bits transmitted without error per unit bandwidth and per unit energy; thus, it reflects the transmission rate, transmission power and outage probability. As the number of BSs increases, the energy efficiency of the proposed TPC increases linearly, and it significantly outperforms the other schemes, because it maintains a lower outage probability and reduces the transmission power while maximizing the minimum rate of the MSs. On the other hand, the scheme using maximum equal power without TPC shows very low energy efficiency, and the SINR-based TPC shows a lower energy efficiency as the interference level increases; additionally, its performance is still closely affected by the target SINR value.

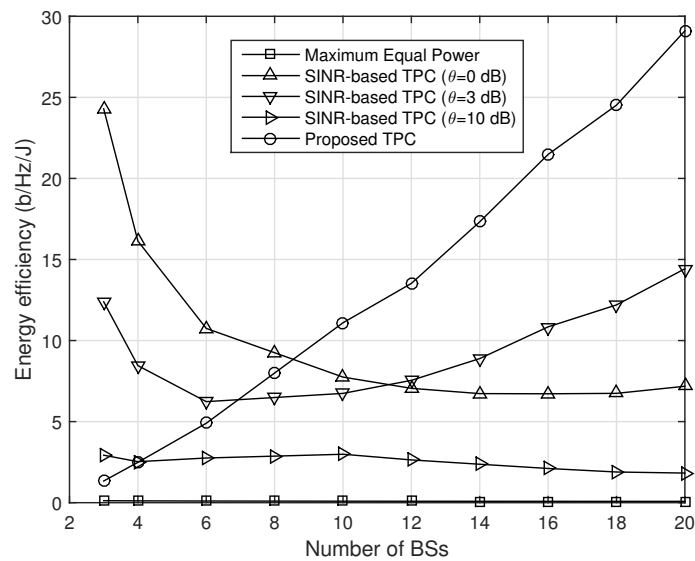


Figure 9. Energy efficiency vs. number of BSs.

## 7. Conclusions

Inspired by flocking behavior in which birds fly together in a group in an energy-efficient way, we have proposed a distributed TPC algorithm in which each MS tries to match its rate to the average rate of the MSs in its adjacent cells by controlling the transmit power of its serving BS, so that the rates of all of the MSs become equal. We verified that this local rate-averaging algorithm achieves an exponential convergence and maximizes the minimum rate of the MSs with the solidarity property. The results showed that the proposed TPC algorithm effectively reduces the power consumption at the BSs while maintaining a low outage probability, which leads to a significant improvement in energy efficiency. Because the proposed TPC algorithm essentially originates in biological flocking behavior, it is simple and distributed, so that we expect it to be applicable to complex cellular networks.

In this paper, we considered only one channel for the TPC. However, the proposed TPC algorithm can also be applied to multiple channels, which are allocated to multiple MSs in a cell. Therefore, our final goal in further study would be to apply the proposed TPC algorithm to the situation of multi-channels and multi-users in conjunction with a scheduling algorithm and to optimize the performance of this joint algorithm with respect to both spectral efficiency and energy efficiency throughout the whole network.

**Acknowledgments:** This research was supported by the Basic Science Research Program through the National Research Foundation of Korea (NRF) funded by the Ministry of Education, Science and Technology (2011-0025424), the MSIP (Ministry of Science, ICT and Future Planning), Korea, under the ITRC (Information Technology Research Center) support program (IITP-2015-H8501-15-1007) supervised by the IITP (Institute for Information & communications Technology Promotion), and the Human Resources Development (No. 20154030200860) of the Korea Institute of Energy Technology Evaluation and Planning (KETEP) grant funded by the Korea government Ministry of Trade, Industry and Energy.

**Author Contributions:** Hyun-Ho Choi contributed by proposing the main idea, deriving the experimental results and writing most of the paper. Jung-Ryun Lee was responsible for theoretical analysis, derivation, coordination and proof reading.

**Conflicts of Interest:** The authors declare no conflict of interest.

## References

1. Han, C. Green radio: Radio techniques to enable energy-efficient wireless networks. *IEEE Commun. Mag.* **2011**, *49*, 46–54.

2. Hasan, Z. Green cellular networks: A survey, some research issues and challenges. *IEEE Commun. Surv. Tutor.* **2011**, *13*, 524–540.
3. Chih-Lin, I.; Rowell, C.; Han, S.; Xu, Z. Toward green and soft: A 5G perspective. *IEEE Commun. Mag.* **2014**, *52*, 66–73.
4. Chung, Y.W. Modeling and performance analysis of state transitions for energy-efficient femto base stations. *Energies* **2015**, *8*, 4629–4646.
5. Wu, Y.; Chen, Y.; Tang, J.; So, D.K.C.; Xu, Z.; Chih-Lin, I.; Ferrand, P.; Gorce, J.-M.; Tang, C.H.; Li, P.-R.; et al. Green transmission technologies for balancing the energy efficiency and spectrum efficiency trade-off. *IEEE Commun. Mag.* **2014**, *52*, 112–120.
6. Chen, Y.; Zhang, S.; Xu, S.; Li, G.Y. Fundamental trade-offs on green wireless networks. *IEEE Commun. Mag.* **2011**, *49*, 30–37.
7. Tan, C.W.; Palomar, D.P.; Chiang, M. Energy-robustness tradeoff in cellular network power control. *IEEE/ACM Trans. Netw.* **2009**, *17*, 912–925.
8. Jiang, C.; Zhang, H.; Ren, Y.; Chen, H.-H. Energy-efficient non-cooperative cognitive radio networks: Micro, meso and macro views. *IEEE Commun. Mag.* **2014**, *52*, 14–20.
9. Das, S.; Viswanathan, H.; Rittenhouse, G. Dynamic load balancing through coordinated scheduling in packet data systems. In Proceedings of the IEEE Infocom, San Francisco, CA, USA, 30 March–3 April 2003.
10. Niu, Z.; Wu, Y.; Gong, J.; Yang, Z. Cell zooming for cost-efficient green cellular networks. *IEEE Commun. Mag.* **2010**, *48*, 74–79.
11. Luo, S. Optimal power and range adaptation for green broadcasting. *IEEE Trans. Commun.* **2013**, *12*, 4592–4603.
12. Javan, M.R.; Sharafat, A.R. Efficient and distributed SINR-based joint resource allocation and base station assignment in wireless CDMA networks. *IEEE Trans. Commun.* **2011**, *59*, 3388–3399.
13. Belke, L.; Kesselheim, T.; Koster, A.M.C.A.; Vocking, B. Comparative study of approximation algorithms and heuristics for SINR scheduling with power control. *Theor. Comput. Sci.* **2014**, *553*, 64–73.
14. Dang, D.N.M.; Hong, C.S.; Lee, S.; Lee, J. A SINR-based MAC protocol for wireless Ad Hoc networks. *IEEE Commun. Lett.* **2012**, *16*, 2016–2019.
15. Seyedi, Y.; Bolouki, E.; Frigon, J.-F. Slow adaptive power control and outage avoidance in composite fading wireless channels. *IEEE Signal Process. Lett.* **2015**, *22*, 930–934.
16. Wang, P.; Kam, P.-Y. Feedback power control with bit error outage probability QoS measure on the rayleigh fading channel. *IEEE Trans. Commun.* **2013**, *61*, 1621–1631.
17. Song, Y.-K.; Kim, D. Convergence and performance of distributed power control algorithms for cooperative relaying in cellular p2p networks. *IEEE Trans. Veh. Technol.* **2010**, *59*, 4645–4651.
18. Papandriopoulos, J.; Evans, J.; Dey, S. Outage-based optimal power control for generalized multiuser fading channels. *IEEE Trans. Commun.* **2006**, *54*, 693–703.
19. Papandriopoulos, J.; Evans, J.; Dey, S. Optimal power control for Rayleigh-faded multiuser systems with outage constraints. *IEEE Trans. Wirel. Commun.* **2005**, *4*, 2705–2715.
20. Kwon, Y.; Hwang, T.; Wang, X. Energy-efficient transmit power control for multi-tier MIMO HetNets. *IEEE J. Sel. Areas Commun.* **2015**, *33*, 2070–2086.
21. Wang, J.T.; Lu, C.C. Throughput-based rate and power control for cognitive radio networks with receive diversity and error control. *IET Commun.* **2012**, *6*, 2848–2854.
22. Xi, Y.; Yeh, E.M. Throughput optimal distributed power control of stochastic wireless networks. *IEEE/ACM Trans. Netw.* **2010**, *18*, 1054–1066.
23. Hanly, S.V. An algorithm for combined cell-site selection and power control to maximize cellular spread spectrum capacity. *IEEE J. Sel. Areas Commun.* **1995**, *13*, 1332–1340.
24. Zhang, H.; Jiang, C.; Beaulieu, N.C.; Chu, X.; Wen, X.; Tao, M. Resource allocation in spectrum-sharing OFDMA femtocells with heterogeneous services. *IEEE Trans. Commun.* **2014**, *62*, 2366–2377.
25. Zhang, H.; Jiang, C.; Beaulieu, N.C.; Chu, X.; Wang, X.; Quek, T.Q.S. Resource allocation for cognitive small cell networks: A cooperative bargaining game theoretic approach. *IEEE Trans. Wireless Commun.* **2015**, *14*, 3481–3493.
26. Zhang, H.; Jiang, C.; Mao, X.; Chen, H. Interference-limited resource optimization in cognitive femtocells with fairness and imperfect spectrum sensing. *IEEE Trans. Veh. Technol.* **2015**, doi:10.1109/TVT.2015.2405538.
27. Cucker, F.; Smale, S. Emergent Behavior in Flocks. *IEEE Trans. Autom. Control* **2007**, *52*, 852–862.



28. Bhandari, V.; Vaidya, N.H. Capacity of multi-channel wireless networks with random channel assignment: A tight bound. In *Technical Report of Illinois University at Urbana Department of Computer Science*; Illinois University: Urbana, IL, USA, 2006; pp. 1–30.
29. Thien, H.P.; Moelyadi, M.A.; Muhammad, H. Effects of leader's position and shape on aerodynamic performances of V flight formation. In *Proceedings of the ICIUS 2007, Bali Indonesia, Indonesia, 24–25 October 2007*.
30. Cutts, C.J.; Speakman, J.R. Energy savings in formation flight of Pink-footed Geese. *J. Exp. Biol.* **1994**, *189*, 251–261.
31. Institute of Electrical and Electronics Engineers (IEEE). IEEE 802.16<sup>TM</sup>-2012. In *IEEE Standard for Air Interface for Broadband Wireless Access Systems*. IEEE: New York, NY, USA, 2012.
32. Kosmanos, D.; Argyriou, A.; Tassioulas, L. Optimizing video quality in dense small-cell wireless networks with packet overhearing. In *Proceedings of the IEEE Global Communications Conference (GLOBECOM), Austin, TX, USA, 8–12 December 2014*.
33. Olfati-Saber, R.; Fax, J.A.; Murray, R.M. Consensus and cooperation in networked multi-agent systems. *Proc. IEEE* **2007**, *95*, 215–233.
34. Chiang, M.; Hande, P.; Lan, T.; Tan, C.W. Power control in wireless cellular networks. *Found. Trends Netw.* **2008**, *2*, 381–533.
35. Choi, H.; Lee, J. Distributed transmit power control for maximizing end-to-end throughput in wireless multi-hop networks. *Springer Wireless Pers. Commun.* **2014**, *74*, 1033–1044.
36. 3GPP, Technical specification group radio access network; further advancements for E-UTRA physical layer aspects (release 9). TR 36.814 v9.0.0, March 2010. Available online: <http://www.3gpp.org/dynareport/36814.htm> (accessed on 9 December 2015).



© 2016 by the authors; licensee MDPI, Basel, Switzerland. This article is an open access article distributed under the terms and conditions of the Creative Commons by Attribution (CC-BY) license (<http://creativecommons.org/licenses/by/4.0/>).